Journal of Alloys and Compounds 509 (2011) 9964–9969

Contents lists available at ScienceDirect

Journal of Alloys and Compounds

journal homepage: www.elsevier.com/locate/jallcom

The influence of short time heat treatment on the structural and magnetic behaviour of $Nd_2Fe_{14}B/\alpha$-Fe nanocomposite obtained by mechanical milling

V. Pop[a,*], S. Gutoiu[a], E. Dorolti[a], O. Isnard[b], I. Chicinaş[c]

[a] Faculty of Physics, Babes-Bolyai University, 400084 Cluj-Napoca, Romania
[b] Institut Néel, CNRS, University Joseph Fourier de Grenoble, BP 166X, 38042 Grenoble, Cédex 9, France
[c] Materials Sciences and Technology Dept., Technical University of Cluj-Napoca, 103-105 Muncii ave., 400641 Cluj-Napoca, Romania

ARTICLE INFO

Article history:
Received 1 July 2011
Received in revised form 1 August 2011
Accepted 3 August 2011
Available online 10 August 2011

Keywords:
Magnetic nanocomposite
Mechanical milling
Hysteresis
Short time annealing
Exchange coupling

ABSTRACT

The structure, microstructure and magnetic properties of $Nd_2Fe_{14}B/\alpha$-Fe nanocomposite obtained after 8 h of high energy milling and different heat treatments are investigated. Two types of annealing have been performed: a conventional heat treatment at 550 °C for 1.5 h is used for comparison with rapid annealing for maximum 3 min at 700, 750 or 800 °C. It is found that these rapid annealing are much more efficient to promote the recrystallisation of the hard phase with a limited grain growth of the soft magnetic phase thus leading to better magnetic properties. Indeed, the best coercive field of 0.55 T was obtained for samples annealed at 700, 750 and 800 °C for 2.5, 1.5 and 1 min respectively. This behaviour is explained by both, a good recovery of crystallinity for the hard phase and relatively small size Fe nanocrystallites. The different heat treatments do not result in significant changes for remanent magnetization, which is between 93 and 107 A m^2/kg. X-ray diffraction patterns were used to follow the evolution of the structure and the microstructure. The magnetic behaviour was checked from hysteresis curves and dM/dH vs. H plots.

1. Introduction

Nanocrystalline ferromagnetic materials exhibit magnetic properties which are interesting from a point of view of fundamental research in magnetism as well as for applications [1–5]. Nanocomposite exchange coupled magnets, spring-magnets, consisting of a fine mixture of hard (high coercivity) and soft (high magnetization) magnetic phases have attracted attention for potential permanent magnet development [6–9]. Additionally to the predicted high energy product of 1090 kJ/m^3 [10], the presence of Fe or Fe based phases in exchange spring magnets is promising for better thermal stabilities, higher corrosion resistance and lower prices. The exchange-spring behaviour can be understood on the basis of the intrinsic parameters of the hard and soft magnetic phases which are coupled by exchange interactions [11,13]. However, the role of the microstructure in the spring mechanism is not well understood [10–16]. The experimental studies, relating to the influence of the microstructure on the hard/soft exchange coupling, have the advantages of different microstructures obtained by dedicated techniques: rapid solidification, mechanical milling/alloying, plastic deformation, thin film multilayers, etc. The importance of the phase composition, including fine substituting/doping elements, is also well exploited in experimental studies. By Ga addition and an appropriate annealing in pulse magnetic field of melt-spun $Nd_2Fe_{14}B/\alpha$-Fe nanocomposite, Zhang et al. obtained a refinement of microstructure and an increase of the magnetic properties [17]. Other researches present some improvement of magnetic properties by Co, Zr [18] or Nb [19] substitutions. In rapidly quenched Nd–Fe–B ribbons, Hirosawa et al. [20] studied the influence of the cooling rate and of the substitution elements, such as Cr and Cu, on the $Fe_3B/Nd_2Fe_{14}B$ formation during rapid solidification. No spectacular improvement of remanence and coercivity has been found up to now by this approach. Dy substitution for Nd has been successfully used to enhance the coercivity in sintered $(Nd_{0.5}Dy_{0.5})_{15}Fe_{77}B_8$ magnet [21]. However, for mechanically milled nanocomposites, the replacement of a small amount of Nd by Dy does not affect the magnetic properties of the nanocomposite [22]. It has been proposed that the main reason of this behaviour could be the fact that Dy substitution results in an increase of the crystallisation temperature of the hard phase, which in turn requires a higher annealing temperature, and thus promotes excessive grain growth for the soft phases and leads to an undesirable microstructure [23]. The increase of the soft magnetic phase percentage, α-Fe, in melt-spun nanocomposite [24] or mechanically milled [25] $Nd_2Fe_{14}B+x\%$ Fe nanocomposite, increase the Curie temperature and improves the corrosion resistance in slightly acidic environment. Mössbauer spectroscopy studies have revealed that in Fe milled powders, a second sextet, with lower mean

* Corresponding author.
E-mail address: viorel.pop@phys.ubbcluj.ro (V. Pop).

0925-8388/$ – see front matter © 2011 Elsevier B.V. All rights reserved.
doi:10.1016/j.jallcom.2011.08.002

hyperfine field, was observed in the spectra and it was attributed to the grain boundaries [26]. Same type of studies on $SmCo_5$/α-Fe exchange spring nanocomposite evidenced also two sextets for Fe. In this case, as result of Co and Fe interdiffusion, the two sextets were attributed to α-Fe(Co) phase and a Fe-richer $Sm(Co, Fe)_5$ phase [27].

One way to improve magnetic properties and exchange coupling between the hard and soft magnetic phases is the optimization of annealing conditions. In mechanically milled samples, the major part of defects and internal stresses could be removed by annealing. The restoration of the crystalline structure of the hard phase by annealing is an important aspect to increase the coercivity. For this type of composites, the recrystallisation temperature of the soft magnetic phase is smaller than the recrystallisation temperature of the hard magnetic phases. Consequently the refinement of the hard phase structure by annealing will come along with an undesirable increase of soft crystallite dimension. In rapidly quenched alloys, Bernardi et al. [28] states that in order to suppress the formation of soft phases, the samples must be annealed at a heating rate of 15–25 K/s. A high heating rate of about 50 K/s or more usually led to the formation of large α-Fe grains. The mechanism responsible for the favoured growth of α-Fe is not explained. A solution could be a rapid annealing for a time of 1–120 s [28].

We succeeded to synthesize $Nd_2Fe_{14}B$/α-Fe and $(Nd, Dy)_2Fe_{14}B$/α-Fe magnetic nanocomposites by mechanical milling and subsequent annealing around of 550 °C for 1.5–2 h [22,29–31]. The milled powders present poor crystallinity and a high defects density. By annealing we intended to recover the crystallinity of the hard phase and, in the same time, to hinder the increase of Fe crystallites during annealing. The weak exchange coupling between Fe and hard magnetic phase was explained by the poor crystallinity of the hard phase. In order to attain simultaneously both objective, a good crystallinity for the hard phase and fine crystallite (smaller than 20 nm) for Fe phase, in this paper we investigate the effects of short time annealing on the microstructure of the hard/soft $Nd_2Fe_{14}B$/α-Fe magnetic composite. The influence of rapid annealing on the structure, microstructure and magnetic properties (H_c, M_r and the strength of interphase exchange coupling) are discussed in comparison with results obtained on nanocomposites annealed at 550 °C for 1.5 h.

2. Experimental

The ingot with $Nd_2Fe_{14}B$ nominal composition was prepared by induction melting under argon atmosphere and annealed at 950 °C for 72 h. The purity of the elements was 99.9%. The ingots were crushed into small pieces and were subsequently mechanically milled for 2 h under argon atmosphere. The powder thus obtained was mixed with elemental NC 100.24 Fe powders (Höganäs) in a weight ratio of 90% $Nd_2Fe_{14}B$/10% Fe. The mixture was mechanically milled (MM) under argon atmosphere using a high-energy planetary mill (Fritsch Pulverisette 4) with the milling vial and the balls made of 440C hardened steel. The milling time was 8 h at a constant speed of the vial of 900 rpm with a ball-to-powder ratio of 10:1. The vials were sealed in an oxygen-free inert environment (argon gas) inside a glove box. Powder handling was carried out always in the same glove box.

In order to investigate the influence of the annealing on the evolution of the hard/soft exchange coupling, the samples of milled powder were sealed in silica tubes. We accomplished for two type of annealing: a conventional heat treatment at 550 °C for 1.5 h and a short time annealing at 700, 750 and 800 °C for times between 0.5 and 3 min. Both type of annealing were performed in the same tubular furnace. For the conventional heat treatment the silica tube with samples were placed in the furnace at the annealing temperature of 550 °C, were maintained for 1.5 h and finally cooled in air. During the heat treatment and the cooling process, the silica tube was continuously evacuated at 10^{-6} mbar. For a better heat transfer, the short time heat treatments were made under argon atmosphere. For this treatment, the samples were placed in the furnace to the annealing temperature (700, 750 or 800 °C) and after a heating period ranging between 0.5 and 3 min the silica tubes containing the samples were removed from the furnace and cooled in water.

The DSC measurements were performed on a Netsch type equipment. The structure and microstructure were checked by X-ray diffraction (XRD) on a Bruker D8 Advance diffractometer with Cu Kα radiation and a Siemens D5000 powder diffractometer using the $K_{\alpha 1}$ radiation of copper ($\lambda = 0.15406$ nm) in the angular interval $2\theta = 20–90°$. The mean sizes of the nanocrystallites were calculated from Full-Width-at-Half-Maximum (FWHM) of the diffraction peaks according to the Scherrer's formula [32]. For this purpose, an internal micro-crystallised standard where also measured to insure a crystallites size accuracy. More details on this analysis can be found elsewhere [33]. The hysteresis curves were recorded at room temperature by the extraction method [34] and by a vibrating sample magnetometer in a continuous magnetic field of up to 10 T. The magnetic particles were blocked in a non magnetic polymer. Considering isolated magnetic particles for hysteresis measurements, we used a demagnetization factor of 1/3 for magnetic data.

3. Results and discussion

In order to optimize the heat treatment of milled powders, we proceed to some thermal analyses of our samples. Fig. 1 shows DSC (differential scanning calorimetry) curves of $Nd_2Fe_{14}B$ sample milled for 6 h. In the heating process, some exothermic peaks are clearly noticed in the sample. The first one, above 200 °C, indicates a release of the milling induced internal stresses. The two peaks at around 440 and 550 °C could be attributed to the recrystallisation of α-Fe and the formation (crystallisation) of Fe_3B phase. The recrystallisation of α-Fe for temperature higher than 500 °C was proved by following the increase of Fe crystallites size as detected from XRD studies [31,35]. The presence of Fe_3B phase in our samples can be linked also to the thermal variation of magnetization ($M(T)$), which show a magnetic phase with a Curie temperature of about 800 K [29]. The relaxation of interface stresses between the particles can also contribute to the exothermic peak at around 440 °C. The presence of α-Fe in $Nd_2Fe_{14}B$ milled sample was also detected by XRD measurements. The crystallisation path observed in some amorphous ribbons take place in two ways: amorphous phase $(Am) \rightarrow Am' + Fe_3B \rightarrow Fe_3B + Nd_2Fe_{23}B_3 \rightarrow Fe_3B + Nd_2Fe_{14}B$, or $(Am) \rightarrow Am' + Fe_3B \rightarrow Fe_3B + Nd_2Fe_{14}B$ [7,20,36–39]. Unlike these situations, in our case for the as-milled composite powders, the thermomagnetic measurements indicate the presence of the Fe_3B phase (T_C around 800 K) in addition to the starting phases $Nd_2Fe_{14}B$ and Fe [29]. The exothermic peak which starts to appear around 700 °C can be attributed to the crystallisation of $Nd_2Fe_{14}B$ magnetic phase [18]. In the cooling process, the DSC signal vs. temperature shows only one transformation before 300 °C. This signal does not indicate any structural modification and it can be attributed to the Curie temperature of $Nd_2Fe_{14}B$ hard phase, which is around 313 °C. To accomplish our objective (crystallised hard magnetic phase and small particle size for the soft magnetic phase), we decided to proceed for rapid annealing at temperatures between 700 and 800 °C. These temperatures are higher than the recrystallisation temperature of $Nd_2Fe_{14}B$ hard magnetic phase and much higher than the recrystallisation temperature of the soft elemental Fe.

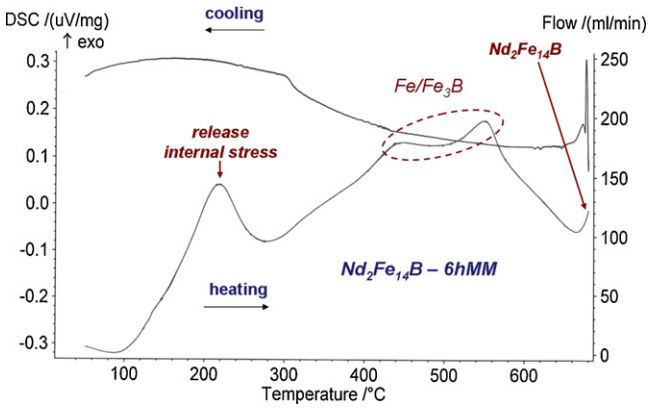

Fig. 1. DSC measurements of $Nd_2Fe_{14}B$ milled for 6 h.

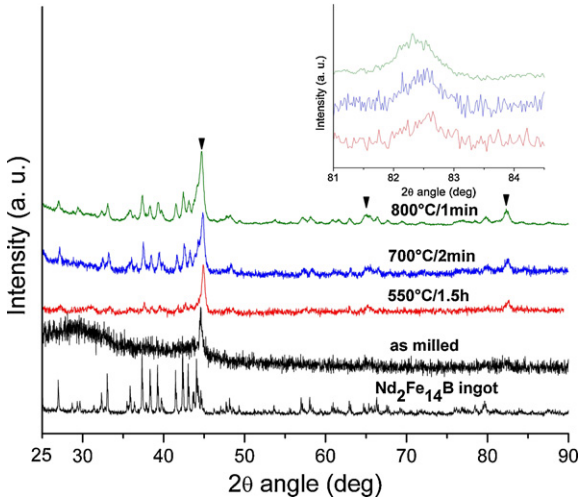

Fig. 2. X-ray diffraction patterns of $Nd_2Fe_{14}B$ + 10% Fe composite samples obtained after 8 h of Mechanical Milling (MM) and annealed at the indicated temperatures and times. A detail of the diffraction peak observed at 82.33° is given in inset. The diffraction pattern of $Nd_2Fe_{14}B$ ingot annealed at 950 °C for 72 h is also given for comparison. The peaks of α-Fe phase are indicated by black triangles.

The X-ray diffraction studies were performed on milled powder samples and also on both type of annealed samples; a conventional heat treatment at 550 °C for 1.5 h and a rapid annealing for times between 0.5 and 2.5 min at temperatures of 700, 750 and 800 °C. As a consequence of the induced internal stresses and decrease of the crystallites size, after 8 h of milling of $Nd_2Fe_{14}B$/α-Fe composite, the width of the diffraction peaks increases and most of them become undetectable, Fig. 2. The diffraction pattern of pure $Nd_2Fe_{14}B$ ingot annealed at 950 °C for 72 h is also given for comparison. The diffraction peaks are well resolved and rather thinner, proving a polycrystalline microstructure. As was found in earlier studies [28–31,35], in order to obtain a good soft/hard exchange coupling, the annealing of milled composite is a critical step. The refinement of the hard phase structure by annealing must avoid the undesirable increase of crystallite size of soft phase. An annealing at 550 °C for 1.5 h restored the characteristic peaks of both phases: $Nd_2Fe_{14}B$ and α-Fe. The peaks of α-Fe phase are indicated by black triangles in Figs. 2 and 3. It is difficult to evidence additional peaks

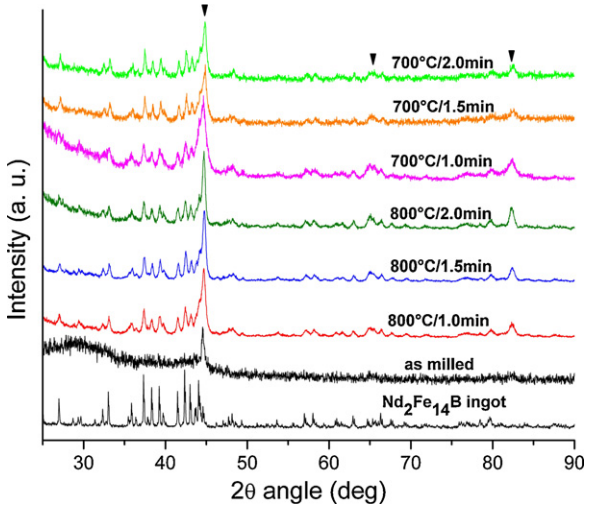

Fig. 3. X-ray diffraction patterns of $Nd_2Fe_{14}B$ + 10% Fe composite samples obtained after 8 h of MM and annealed at 700 and 750 °C for 1, 1.5 and 2 min. The diffraction pattern of $Nd_2Fe_{14}B$ ingot annealed at 950 °C for 72 h is also given for comparison. The peaks of α-Fe phase are indicated by black triangles.

Table 1
The crystallites mean size of α-Fe phase in a $Nd_2Fe_{14}B$ + 10% Fe composite milled for 8 h and annealed at different temperatures and times. The crystallite size has been calculated according to Scherrer's formula from XRD patterns obtained with Cu $K_{\alpha 1}$ radiation.

Annealing temperature (°C)	Annealing time (min)	FWHM (°)	*D* (nm)
800	1.0	0.61	17 (±2)
	1.5	0.50	21 (±2)
	2.0	0.43	25 (±2)
700	1.0	0.88	12 (±2)
	1.5	0.77	14 (±2)
	2.0	0.66	16 (±2)
550	90	0.40	26 (±2)

of Fe_3B phase. This indicates that this remains a minority phase. The influence of annealing on the 8 h milled samples, for conventional heat treatment at 550 °C and a rapid annealing at 700 and 800 °C is illustrated in Fig. 2. For rapid annealing, we observed a net improving of the crystallinity of the hard phase in comparison with conventional annealing. Another noticeable result is the larger increase of the intensity of the peaks of the $Nd_2Fe_{14}B$ type phase comparison with that of the soft phase. This indicates that rapid annealing performed here are efficient to lead to the growth of the hard phase without excessive increase of the crystallites of soft magnetic one. More the width of the diffraction peaks of α-Fe are a slightly wider for short time annealing, see in inset of Fig. 2 as example the peak from 82.33°. It appears that by rapid annealing we succeed to recover the crystallinity of hard magnetic phase without a net increasing of α-Fe crystallites sizes. This behaviour is explained by the fact that the annealing temperatures for rapid heat treatments are higher than the recrystallisation temperature of $Nd_2Fe_{14}B$ hard magnetic phase. The conservation of small size of Fe crystallites can be understood by the short time of annealing. This assumption is supported also by the rapid increase of the size of Fe crystallites by increasing the annealing time for short time annealing. The XRD patterns of samples milled 8 h and rapidly heat treated at 700 and 800 °C, for 1, 1.5 and 2 min are given in Fig. 3. For all the samples the characteristic peaks of $Nd_2Fe_{14}B$ hard phase are well resolved. This fact attests a good crystallinity of hard phase for both annealing at 700 and 800 °C respectively. The characteristic peaks of α-Fe phase are large, proving that these heat treatments do not produce a great increase of Fe crystallites. In comparison with the peaks of $Nd_2Fe_{14}B$ ingot, the composite samples milled for 8 h and rapidly annealed at 700 or 800 °C present broader peaks, proving the small crystallites obtained after milling and annealing.

The nanocrystallites mean sizes of α-Fe crystallites in $Nd_2Fe_{14}B$/α-Fe composite, milled for 8 h and annealed, calculated from diffraction peak $2\theta = 82.33°$, according to Scherrer's formula, are given in Table 1. For annealed samples, classical and rapid annealing, as shown in Fig. 1 we consider that the second-order internal stresses were removed; consequently, their contribution to the FWHM was neglected. For all rapid heat treatment up to 2 min the crystallite size are smaller than 25 nm. The small size of the crystallites obtained for a sample annealed at 700 °C for 1 min: 12 nm, entitles us to believe that no significant recrystallisation takes place during these annealing. Moreover, the same conclusion can be drawn also for short annealing (up to 1 min) at 800 °C. It is important to note that the sizes of Fe crystallites in samples annealed at 550 °C for 1.5 h are 26 nm, being bigger than the Fe crystallites obtained after rapid annealing at higher temperature. This large crystallite size will results in a poor hard soft coupling for samples obtained after long time annealing at 550 °C in comparison with samples obtained by short time annealing at 700–800 °C.

The soft/hard exchange coupling was studied from the hysteresis loops and from *dM/dH* vs. *H* curves. The demagnetization curves

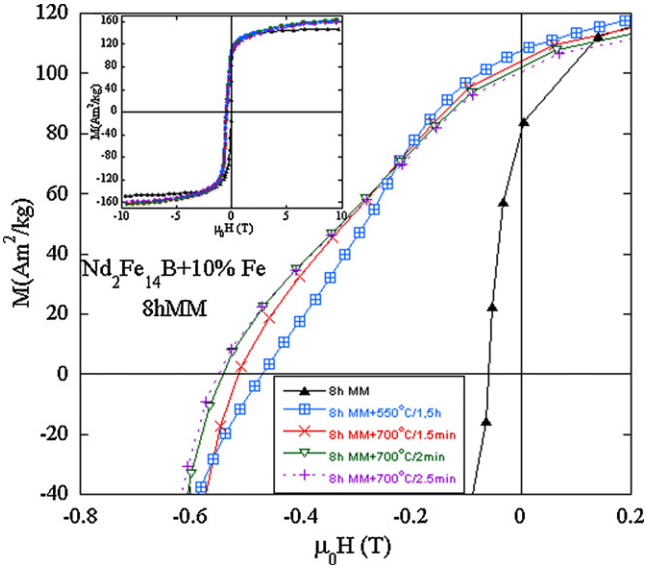

Fig. 4. Room temperature demagnetization curves recorded for the $Nd_2Fe_{14}B$ + 10% Fe composite milled 8 h, as-milled samples and annealed samples at 550 and 700 °C for times indicated in the figure. The corresponding hysteresis curves are given in inset.

for $Nd_2Fe_{14}B/\alpha$-Fe composites milled for 8 h and rapidly annealed at 700 and 750 °C for different times are plotted in Fig. 4 (8 h MM+ 700 °C/*x* min) and Fig. 5 (8 h MM+ 750 °C/*x* min) respectively. The demagnetization curves for 8 h milled samples, 8 h MM, and samples annealed at 550 °C for 1.5 h, 8 h MM+ 550 °C/1.5 h, are given also for comparison. The saturation behaviour is illustrated in the inset of Figs. 4 and 5 for the hysteresis loops between ±10 T. From both figures we can observe an obvious improving of the coercivity and remanence after annealing, either conventional or rapid annealing. Furthermore, for samples obtained by rapid annealing the coercive field is higher than that for samples obtained by classical annealing. On the contrary, the remanence magnetization is slightly larger for the samples obtained by conventional annealing. The remanent magnetization decreases slowly by increasing the

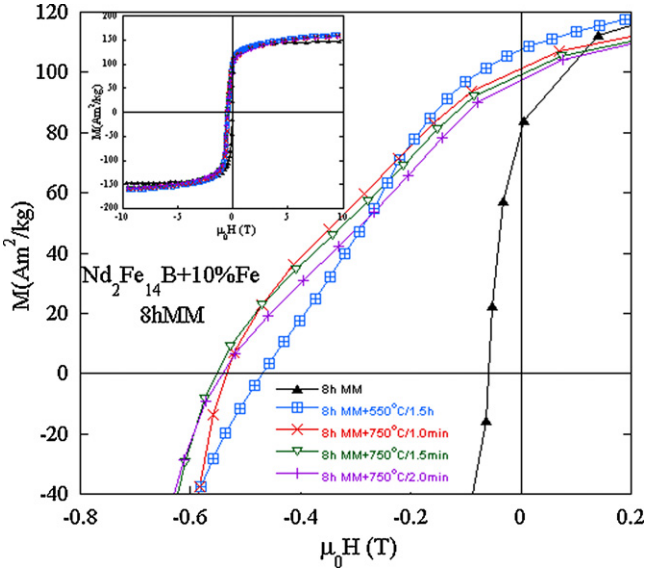

Fig. 5. Room temperature demagnetization curves recorded for the $Nd_2Fe_{14}B$ + 10% Fe composite milled 8 h, as-milled samples and annealed samples at 550 and 750 °C for times indicated in the figure. The corresponding hysteresis curves are given in inset.

Table 2
Coercive field and remanent magnetization of $Nd_2Fe_{14}B/\alpha$-Fe composite samples obtained after 8 h of MM and annealed at 550, 700, 750 and 800 °C for the indicated times. For comparison other data taken from the literature [24,41–44] are also given.

Annealing temperature (°C)	Annealing time (min)	$\mu_0 H_c$ (T)	M_r (A m²/kg)
700	0.5	0.062	106
	1.0	0.417	104
	1.5	0.510	103
	2.0	0.541	102
	2.5	0.550	100
750	0.5	0.077	
	1.0	0.534	101
	1.5	0.555	99
	2.0	0.542	97
	2.5	0.537	100
800	1.0	0.544	98
	1.5	0.543	96
	2.0	0.497	93
	2.5	0.478	94
550	90.0	0.470	107
0	0.0	0.058	81
$Nd_2Fe_{14}B$ + 10 wt% α-Fe; milling and hot-pressing at 650 °C for 30 min [24]		0.500	80
$Nd_7DyFe_{87.5}B_{4.5}$ (30% α-Fe); melt spinning and annealing at 615 °C/2 min [41]		0.494	115
$Nd_{8.4}Fe_{87.1}B_{4.5}$; mechanical alloying and annealing 650 °C/20 min [42]		0.350	110
$1-x$ wt% $Nd_{8.55}Fe_{84.49}W_{0.60}B_{6.36}$ + x wt% Co; mechanical alloying + annealing at 675 °C [43]		0.515	107
$Nd_2Fe_{14}B$ + 10% α-Fe; milled for 48 h and annealed at 650–750 °C [44]		0.600	94

temperature or the time of rapid annealing. This behaviour could be connected with the decrease of the exchange strength of α-Fe phase, given by the slight increase of Fe crystallites. The values of coercive fields and remanent magnetizations are given in Table 2 for the studied samples. This behaviour is in good agreement with the structural and microstructural behaviour evidenced before; the diffraction patterns showed a better crystallinity of hard phase after rapid annealing than after conventional annealing at 550 °C for 1.5 h. The demagnetization curves for rapid annealed samples are smoother than that for samples annealed at 550 °C for 1.5 h. This behaviour is explained by the smaller Fe crystallites obtained in rapid annealed samples, Table 1. For samples annealed at 700 °C we can observe a progressive increasing of coercive field by increasing of the annealing time. However saturation can be seen for 2.5 min of annealing. The coercive field is maximum for the sample annealed for 1.5 min at 750 °C. For higher annealing temperature we expect a decreasing of the optimum annealing time. Indeed for annealing at 800 °C the maximum coercive field is obtained for 1 min of heat treatment, Table 2. For 2 min of annealing a decoupling between the hard and the soft magnetic phases can be seen from the demagnetization curves in Fig. 6. This behaviour is better evidenced from *dM/dH* vs. *H* curves, Fig. 6, where, at lower fields, a second peak emerges for the 2 min annealed sample. In Fig. 7 we present *dM/dH* vs. *H* curves for the samples with the higher coercivity (annealed at 700, 750 and 800 °C for 2.5, 1.5 and 1 min respectively) and samples annealed at 800 °C for 2 min, annealed at 550 °C for 1.5 h and as-milled sample. The as-milled samples present only one peak at very low field. This behaviour proves the bad coercivity of milled composite which can be explained by the poor crystallinity of hard phase after milling. The *dM/dH* vs. *H* curves for samples annealed at 700, 750 and 800 °C for 2.5, 1.5 and 1 min respectively present a big and sharp peak at around 0.6 T and also a shoulder at around 0.16 T. The important peak at 0.6 T is given by the hard/soft composite well coupled by exchange interactions. The peak at around 0.16 T can be attributed to the coupled Fe_3B and α-Fe phases. This assumption is based on the previous observation from DSC measurements and

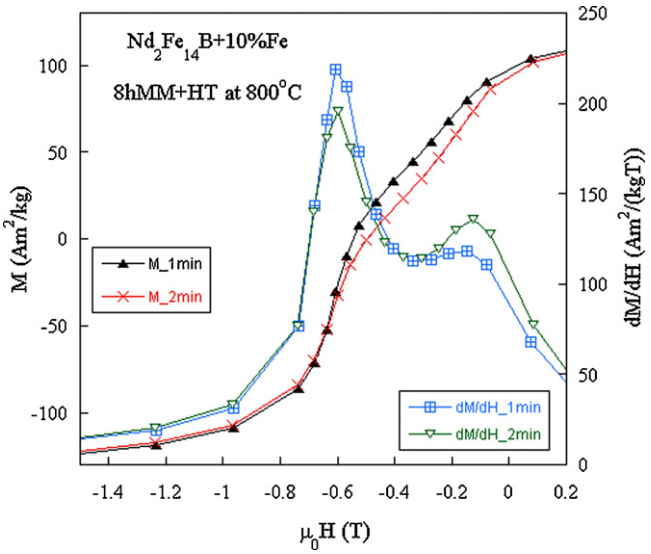

Fig. 6. Room temperature demagnetization curves and *dM/dH* vs. *H* curves recorded for the $Nd_2Fe_{14}B$ + 10% Fe composite milled for 8 h and annealed at 800 °C for 1 and 2 min.

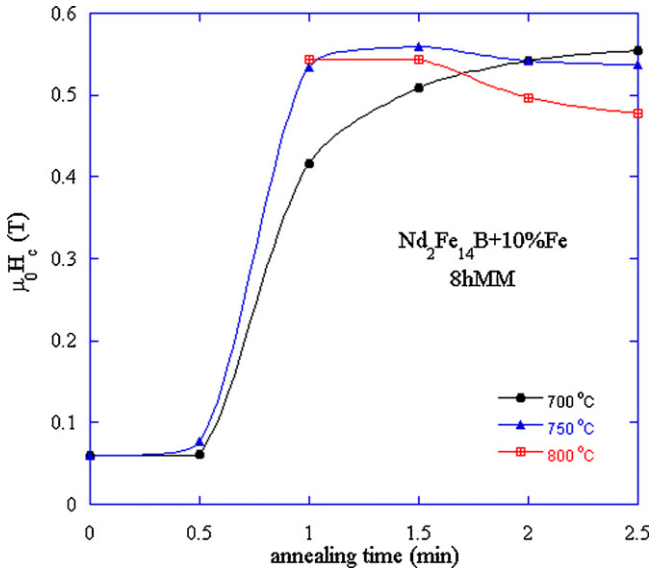

Fig. 8. Coercive field vs. annealing times for $Nd_2Fe_{14}B$ + 10% Fe composite milled for 8 h and annealed at 700, 750 and 800 °C.

on the literature data which show that Fe_3B gives a magnetic phase with coercivity around 0.2 T [40].

The samples rapidly annealed at 800 °C for 2 min and conventionally annealed at 550 °C for 1.5 h present a lower peak at 0.6 T and second supplementary peaks at low field in the *dM/dH* vs. *H* curves. The increase of the second peak at low field proves that for these last annealing it is possible to initiate the crystallisation of a semi-hard magnetic phase such as Fe_3B phase. To understand this behaviour, it is worth to note also that the crystallite sizes are bigger for sample obtained after conventionally annealing at 550 °C for 1.5 h. Indeed the crystallite sizes increase from 17 to 25 nm when the time of annealing, at 800 °C, increases from 1 to 2 min, see Table 1. The evolution of the coercive field vs. annealing conditions is illustrated in Fig. 8. By this preparation method, after 8 h of dry milling and different heat treatments, a maximum coercivity of 0.59 T can be reached. The importance of the annealing time and temperature is well illustrated in Fig. 8. Comparable coercivity of the magnetic nanocomposite can be attained for shorter annealing time when increasing the annealing temperature. Magnetic properties of $Nd_2Fe_{14}B/\alpha$-Fe (10 wt% of Fe) studied nanocomposites, obtained after 8 h of mechanical milling and different annealing, are in the same range as other reported data [25,41–44], Table 2.

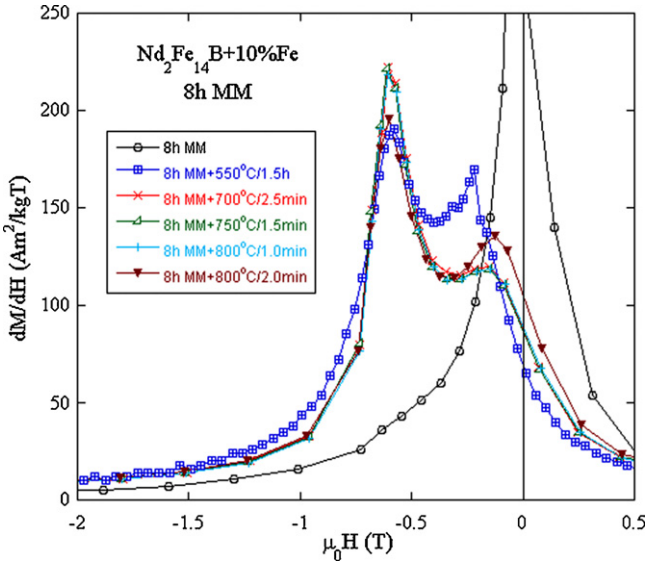

Fig. 7. Room temperature *dM/dH* vs. *H* curves recorded for the $Nd_2Fe_{14}B$ + 10% Fe composite milled for 8 h and annealed at 550, 700, 750 and 800 °C for the indicated times.

4. Conclusions

$Nd_2Fe_{14}B/\alpha$-Fe nanocomposites have been obtained after 8 h of mechanical milling and different annealing: conventional and rapid heat treatments. The influence of the annealing conditions on the structural and magnetic behaviour of mechanically milled $Nd_2Fe_{14}B/\alpha$-Fe composites has been studied. The diffraction peaks of hard magnetic phase are broadened by milling and the peaks almost disappear for 8 h of milling. The characteristic diffractions peaks of $Nd_2Fe_{14}B$ phase are restored during conventional heat treatment at 550 °C for 1.5 h or short time annealing at 700, 750 or 800 °C. The annealing induces also a refinement of the α-Fe structure. DSC studies suggest the crystallisation of Fe_3B phase also. Because of the partial superposition of $Nd_2Fe_{14}B$ and Fe_3B phase it was difficult to evidence the presence of Fe_3B phase from XRD measurements. The Fe crystallites sizes of short annealed samples are smaller than the crystallite sizes of samples obtained after heat treatment at 550 °C for 1.5 h. To summarize, it is found that these rapid annealing approach tested here is more efficient to promote the recrystallisation of the hard Nd-Fe-B phase without leading to an excessive grain growth of the soft magnetic phase. This favours the obtention of better magnetic properties.

The best interphase coupling with a coercivity of 0.47 T was obtained in classical annealed samples after a heat treatment at 550 °C for 1.5 h. By rapid annealing, the coercivity increases by about 20%. A better coercivity of 0.55 T (see Table 2) is obtained for samples annealed at 700, 750 and 800 °C for 2.5, 1.5 and 1 min respectively. After rapid annealing, the increasing of coercivity is not accompanied by an increasing of the remanence. This behaviour results from a weakness in the interphase coupling and probably from the presence of Fe_3B phase as was evidenced from *dM/dH* vs. *H* curves. However, for classical annealed samples, the interphase exchange coupling is better for the 6 h milled samples than in samples obtained after 8 h of milling. Consequently further

investigations are in progress on the influence of short time annealing on the 6 h milled samples.

Acknowledgements

The authors are grateful to M. Valeanu and C. Popa, for DSC measurements and discussions. This work was supported by the Romanian Ministry of Education and Research, Grant PNCD II-72-186/2008 and the POSDRU 89/1.5/S/60189 Postdoctoral Programs.

References

[1] O. Gutfleisch, A. Bollero, A. Handstein, D. Hinz, A. Kirchner, A. Yan, K.H. Muller, L. Schultz, J. Magn. Magn. Mater. 242–245 (2002) 1277–1283.
[2] R. Hasegawa, J. Magn. Magn. Mater. 304 (2006) 187–191.
[3] G.C. Hadjipanayis, J. Magn. Magn. Mater. 200 (1999) 373–391.
[4] Y. Yoshizawa, S. Oguma, K. Yamauchi, J. Appl. Phys. 64 (1988) 6044.
[5] G. Herzer, M. Vazquez, M. Knobel, A. Zhukov, R. Reininger, H.A. Davies, R. Grossinger, J.L. Sanchez, J. Magn. Magn. Mater. 294 (2005) 252–266.
[6] E.F. Kneller, R. Hawig, IEEE Trans. Magn. 27 (1991) 3588–3600.
[7] R. Coehoorn, D.B. de Mooij, C. De Waard, J. Magn. Magn. Mater. 80 (1989) 101–104.
[8] R. Coehoorn, D.B. de Mooij, J.P.W.B. Duchateau, K.H.J. Buschow, J. Phys. (Paris) Colloq. 49 (1988) C8–C669.
[9] P. Saravanan, R. Gopalan, R. Priya, P. Ghosal, V. Chandrasekaran, J. Alloys Compd. 477 (2009) 322–327.
[10] R. Skomski, J. Appl. Phys. 76 (1994) 7059.
[11] E.E. Fullerton, J.S. Jiang, S.D. Bader, J. Magn. Magn. Mater. 200 (1999) 392–404.
[12] R. Fischer, T. Schrefl, H. Kronmüller, J. Fidler, J. Magn. Magn. Mater. 153 (1996) 35–49.
[13] T. Schrefl, J. Fidler, H. Kronmüller, Phys. Rev. B 49 (1994) 6100–6110.
[14] E.E. Fullerton, J.S. Jiang, M. Grimsditch, C.H. Sowers, S.D. Bader, Phys. Rev. B 58 (1998) 12193–12200.
[15] R. Skomski, J. Phys.: Condens. Matter 15 (2003) R841–R896.
[16] R. Skomski, J.M.D. Coey, Permanent Magnetism, Institute of Physics Publishing, Bristol, 1999.
[17] S. Zhang, H. Xu, X. Tan, J. Ni, X. Hou, Y. Dong, J. Alloys Compd. 459 (2008) 41–44.
[18] S.Y. Zhang, H. Xu, J.S. Ni, H.L. Wang, X.L. Hou, Y.D. Dong, Physica B 393 (2007) 153–157.
[19] W. Zhanyong, L. Wenqing, Z. Bangxin, N. Jiansen, X. Hui, F. Yongzheng, J. Minglin, Physica B 404 (2009) 1321–1325.
[20] S. Hirosawa, Y. Shigemoto, T. Miyoshi, H. Kanekiyo, Scripta Mater. 48 (2003) 839–844.
[21] M. Sagawa, S. Hirosawa, K. Tokuhara, J. Appl. Phys. 61 (1987) 3559.
[22] E. Dorolti, V. Pop, O. Isnard, D. Givord, I. Chicinas, J. Optoelectron. Adv. Mater. 9 (2007) 1474–1477.
[23] G.C. Hadjipanayis, L. Withanawasam, R.F. Krause, IEEE Trans. Magn. 31 (1995) 3596–3601.
[24] L.H. Lewis, D.O. Welch, V. Panchanathan, J. Magn. Magn. Mater. 175 (1997) 275–278.
[25] M. Rada, J. Lyubina, A. Gebert, O. Gutfleisch, L. Schultz, J. Magn. Magn. Mater. 290–291 (2005) 1251–1254.
[26] A. Guittoum, A. Layadi, H. Tafat, N. Souami, J. Magn. Magn. Mater. 322 (2010) 566–571.
[27] J.M. Le Breton, R. Lardé, H. Chiron, V. Pop, D. Givord, O. Isnard, I. Chicinaş, J. Phys. D: Appl. Phys. 43 (2010) 085001.
[28] J. Bernardi, T. Schrefl, J. Fidler, Th. Rijks, K. de Kort, V. Archambault, D. Pere, S. David, D. Givord, J.F. O'Sullivan, P.A.I. Smith, J.M.D. Coey, U. Czernik, M. Gronefeld, J. Magn. Magn. Mater. 219 (2000) 186–198.
[29] O. Isnard, D. Givord, E. Dorolti, V. Pop, L. Nistor, A. Tunyagi, I. Chicinaş, J. Optoelectron. Adv. Mater. 10 (2008) 1819–1822.
[30] S. Gutoiu, E. Dorolti, O. Isnard, I. Chicinas, V. Pop, Proc. Materiaux 2010 Congrès, Nantes, France, 2010, pp. 8–22.
[31] S. Gutoiu, E. Dorolti, O. Isnard, I. Chicinaş, V. Pop, J. Optoelectron. Adv. Mater. 12 (2010) 2126–2131.
[32] P. Scherrer, Göt Nachr. 2 (1918) 98.
[33] V. Pop, O. Isnard, I. Chicinas, J. Alloys Compd. 361 (2003) 144–152.
[34] A. Barlet, J.C. Genna, P. Lethuillier, Cryogenics 31 (1991) 801–805.
[35] V. Pop, O. Isnard, I. Chicinas, D. Givord, J.M. Le Breton, J. Optoelectron. Adv. Mater. 8 (2006) 494–500.
[36] H. Sheng, X. Zeng, J. Zou, S. Xie, J. Rare Earths 28 (2010) 447–450.
[37] B.-g. Shen, L.-y. Yang, L. Cao, H.-y. Yang, J.-g. Zhao, F.-m. Yang, J. Magn. Magn. Mater. 104–107 (1992) 1281–1282.
[38] M. Rajasekhar, D. Akhtar, M. Manivel Raja, S. Ram, J. Magn. Magn. Mater. 320 (2008) 1645–1650.
[39] S. Nasu, T. Hinomura, S. Hirosawa, H. Kanekiyo, Physica B 237 (1997) 283–285.
[40] L. Shandong, B. Hong, X. Guozhi, Z. Wei, Z. Fengming, G. Benxi, Z. Jianrong, L. Mu, D. Youwei, J. Magn. Magn. Mater. 282 (2004) 202–205.
[41] W. Chen, X. Zhao, J.J. Hu, A.J. Li, Y. Tian, G.D. Tang, R.W. Gao, M.G. Zhu, X.M. Li, W. Li, J. Magn. Magn. Mater. 306 (2006) 51–54.
[42] B.Z. Cui, X.K. Sun, W. Liu, Z.D. Zhang, D.Y. Geng, X.G. Zhao, J. Phys. D: Appl. Phys. 33 (2000) 338–344.
[43] C. You, X.K. Sun, W. Liu, B. Cui, X. Zhao, Z. Zhang, J. Phys. D: Appl. Phys. 33 (2000) 926–931.
[44] W. Gong, G.C. Hadjipanayis, R.F. Krause, J. Appl. Phys. 75 (1994) 6649.